Photophysical properties and intracellular imaging of water-soluble porphyrin dimers for two-photon excited photodynamic therapy†

Marina K. Kuimova,[a] Hazel A. Collins,[b] Milan Balaz,[b] Emma Dahlstedt,[b] James A. Levitt,[c] Nicolas Sergent,[c] Klaus Suhling,[c] Mikhail Drobizhev,[d] Aleksander Rebane,[d] Harry L. Anderson*[b] and David Phillips*[a]

Receipt/Acceptance Data **[DO NOT ALTER/DELETE THIS TEXT]**
Publication data **[DO NOT ALTER/DELETE THIS TEXT]**
DOI: 10.1039/b000000x [DO NOT ALTER/DELETE THIS TEXT]

We have investigated the photophysical properties and intracellular behaviour of a series of hydrophilic conjugated porphyrin dimers. All the dimers exhibit intense linear absorption at 650–800 nm and high singlet oxygen quantum yields (0.5–0.9 in methanol), as required for an efficient sensitiser for photodynamic therapy (PDT). They also exhibit fluorescence at 700–800 nm, with fluorescence quantum yields of up to 0.13 in methanol, and show extremely large two-photon absorption maxima of 8,000–17,000 GM in the near-IR. The dimers aggregate in aqueous solution, but aggregation is reduced by binding to bovine serum albumin (BSA), as manifested by an increase in fluorescence intensity and a sharpening in the emission bands. This process can be regarded as a model for the interaction with proteins under physiological conditions. Confocal fluorescence microscopy of live cells was used to monitor the rate of cellular uptake, intracellular localisation and photostability. Porphyrin dimers with positively charged substituents partition into cells more efficiently than the negatively charged dimers. The photostability of these dimers, in living cells, is significantly better than that of the clinical photosensitiser verteporfin. Analysis of the photophysical parameters and intracellular imaging data indicates that these dimers are promising candidates for one-photon and two-photon excited PDT.

Introduction

Photodynamic therapy (PDT) is a light-activated treatment which is used in the clinic to destroy diseased tissues,[1,2] and is in trials for the eradication of localised bacterial infections.[3] PDT drugs (or *photosensitisers*) achieve their therapeutic effect by generating a cytotoxic species in the presence of light, by either electron-transfer (Type I) or energy-transfer (Type II) processes. The majority of photosensitisers are tetrapyrroles or porphyrinoids; these drugs cause cell death by transferring energy to oxygen, producing the highly reactive singlet excited state of molecular oxygen, $^1O_2$ ($^1\Delta_g$ state).

An efficient PDT photosensitiser requires a favourable combination of the following factors: (i) light absorption at wavelengths which penetrate effectively into biological tissue (700–950 nm),[4] (ii) a high quantum yield for singlet oxygen generation (ϕ_Δ), (iii) efficient uptake into the diseased tissues, and (iv) localisation in regions of the cell which are vulnerable to singlet oxygen damage. Here we focus on these four factors, although there are also other important requirements such as low dark toxicity and good pharmacokinetics.

Photofrin® was the first photosensitiser approved for clinical use.[1] However it has several drawbacks including relatively low absorption in the tissue transparency window (ε = 3200 cm^{-1} M^{-1} at 630 nm),[5] slow clearance from the body and prolonged skin photosensitivity. These limitations are reduced in the second generation of photosensitisers[1] which include chlorins (*e.g.* chlorine e6, tetrahydroxy-tetraphenylchlorin formulated as Foscan® or verteporfin formulated as Visudyne®), bacteriochlorins (such as TOOKAD®) and phthalocyanines. The singlet oxygen quantum yields of clinical photosensitisers vary from 0.1 to 1.0 and are strongly solvent dependent.[6] The efficiency of singlet oxygen generation by a hydrophobic sensitiser can be severely compromised in an aqueous environment due to aggregation, thereby leading to a lower PDT efficiency. The cellular response to PDT also depends on the primary organelle targeted by the photosensitiser.[7,8] Most clinical photosensitisers induce apoptosis, generally via direct damage to the mitochondria;[7] however, a secondary apoptotic response can be achieved by initial damage to the lysosomes.[7] Photofrin®, on the other hand, localises in cell membranes and PDT with this photosensitiser is reported to induce necrosis.[9]

The cytotoxic response during PDT is strictly limited to the irradiated area due to the high reactivity and short lifetime of the photochemically produced intermediates. However healthy tissues which contain the photosensitiser may be damaged if they lie in the beam path. An additional degree of spatial selectivity may be achieved by two-photon excited photodynamic therapy[10-12] due to the quadratic dependence of the absorption probability on the light intensity. This approach has great potential for the treatment of conditions where precise differentiation between healthy and diseased tissue is necessary, such as during the treatment of wet age-

[a] *Chemistry Department, Imperial College London, Exhibition Road, London SW7 2AZ, UK. E-mail: d.phillips@imperial.ac.uk;* [b] *Department of Chemistry, Oxford University, Chemistry Research Laboratory, Oxford OX1 3TA, UK. E-mail: harry.anderson@chem.ox.ac.uk;*
[c] *Department of Physics, King's College London, Strand, London WC2R 2LS, UK;*
[d] *Department of Physics, Montana State University, Bozeman, Montana 5917-384, USA.*

† Electronic Supplementary Information (ESI) available: additional spectroscopic and imaging data. See http://dx.doi.org/10.1039/b000000x/

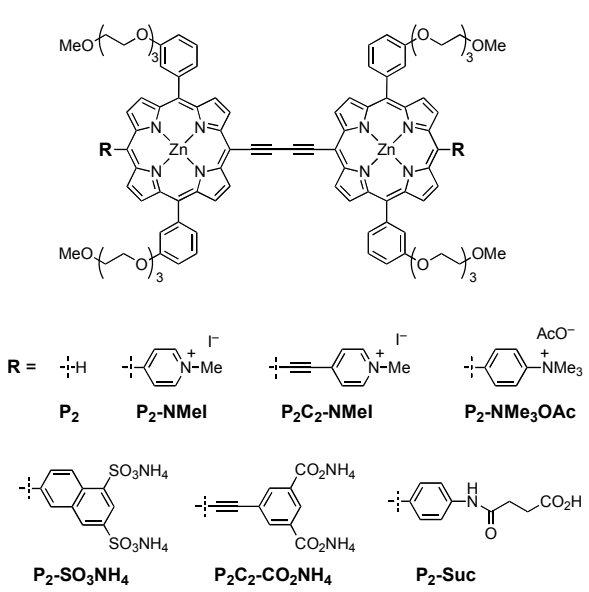

Fig. 1 The structure of the conjugated porphyrin dimers under study.

related macular degeneration (wet AMD) where abnormal blood vessels are targeted in the retina.[13,14]

Several clinical photosensitisers have been reported to induce *in vitro* PDT effects under two-photon excitaton[15,16] with therapeutic efficiencies which are proportional to their cross-sections for two-photon absorption (TPA).[16] Two-photon excitation of verteporfin has been recently employed to occlude fine blood vessels in the chick embryo chorioallantoic membrane (CAM).[17] However all the clinical photosensitisers which have been tested so far are inefficient two-photon chromophores, that is, they possess low TPA cross-sections, δ. For example, $\delta = 10$ GM (1 GM = 10^{-50} cm^4 s photon^{-1}) at 800 nm for Photofrin®,[15] 1.0 GM at 800 nm for protoporphyrin IX (the product of 5-aminevulinic acid synthesis)[11] and 50 GM at 900 nm for verteporfin.[16] Thus the utility of existing photosensitisers for *in vivo* two-photon excited PDT is limited.

For clinical applications of two-photon excited PDT, there is a need for efficient two-photon chromophores that fulfil the biological and photophysical requirements listed above. The design and synthesis of photosensitisers with high two-photon cross-sections is currently an area of intense research effort.[18-25] Conjugated porphyrin oligomers have attracted attention due to their strong two-photon absorption ($\delta \approx$ 5,000–25,000 GM) and straightforward synthesis.[20,26,27] We recently reported the design of a hydrophilic porphyrin dimer with a very large TPA cross-section, **P_2C_2-NMeI**, Fig. 1.[28,29] This photosensitiser was used successfully to close 40 ± 5 μm blood vessels in the mouse window chamber model by applying two-photon excitation.[28]

This article explores the photophysical properties and intracellular uptake of a series of amphiphilic conjugated porphyrin dimers, related to **P_2C_2-NMeI**, see Fig. 1. We assess the properties pertinent for both one- and two-photon excitation PDT, including their absorption spectra and singlet oxygen quantum yields. We also measure their fluorescence quantum yields, relevant for *in vitro* and *in vivo* imaging. Using fluorescence microscopy, we monitor the accumulation of the photosensitisers in epithelial human ovarian adenocarcinoma cells (SK-OV-3) and assess their rate of uptake, intracellular localisation and photostability.

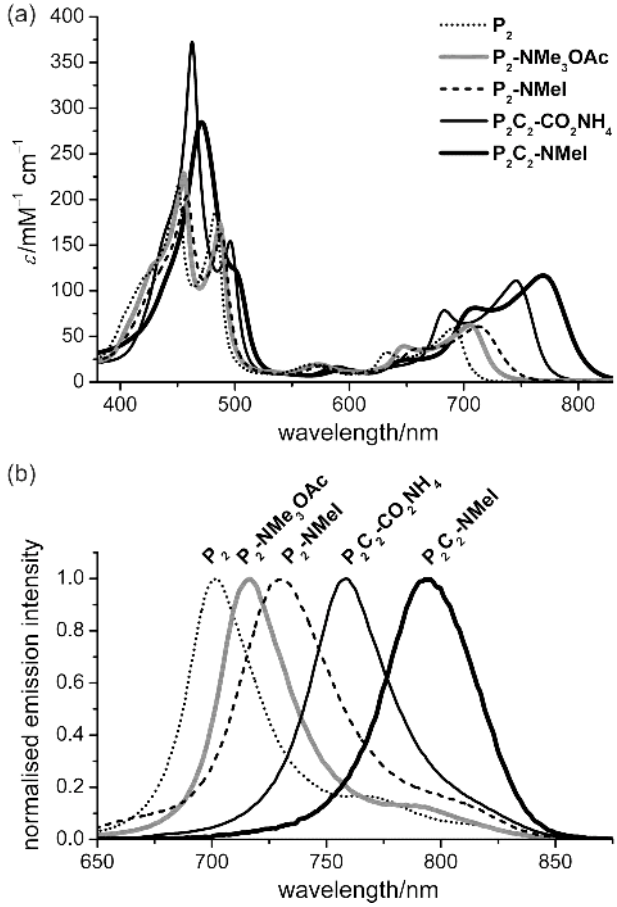

Fig. 2 (a) Absorption spectra of porphyrin dimers in DMF solution containing 0.5% pyridine and (b) fluorescence spectra in DMSO: **P_2** (black dots), **P_2-NMeI** (black dash), **P_2C_2-NMeI** (black bold), **P_2-NMe_3OAc** (grey bold), **P_2C_2-CO_2NH_4** (black narrow).

Results and discussion

Solubility Behaviour

Conjugated porphyrin dimers without polar substituents are hydrophobic and are completely insoluble in water, rendering them unsuitable for PDT. We have designed and synthesised a series of hydrophilic porphyrin dimers,[29] Fig. 1, modified with triethyleneglycol moieties. These substituents alone are insufficient to provide water-solubility, as we found that **P_2** precipitates slowly (48 hours) from aqueous solutions containing up to 2% DMSO. Therefore the hydrophilicity of the conjugated porphyrin dimers was increased by substituting the terminal porphyrin *meso*-positions with either cationic or anionic aryl groups. Visual inspection confirms that 1 μM aqueous solutions of all the charged porphyrin dimers containing up to 2% DMSO are stable for longer than 48 hours. The synthesis of all the compounds shown in Fig. 1 is reported in the preceding article.[29]

Linear Absorption and Fluorescence Spectra

The spectroscopic properties of all the conjugated dimers shown in Fig. 1 have been studied in organic solvents and aqueous solutions. The dimers can be divided into two groups according to the size of their conjugated π-system. Dimers **P_2-NMeI, P_2-**

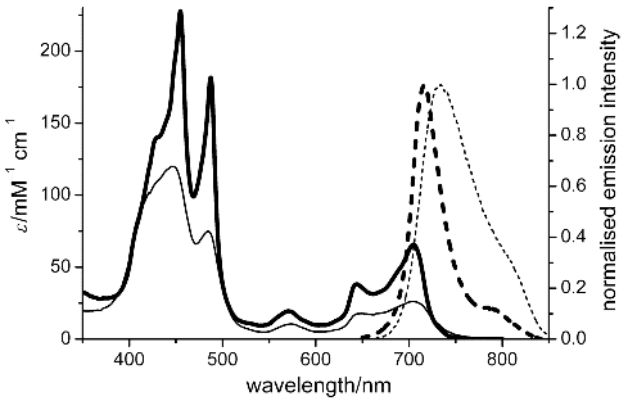

Fig. 3 Absorption (solid lines) and normalised fluorescence spectra (dashed lines) of porphyrin dimer **P_2-NMe_3OAc** in DMSO (bold lines) and in aqueous solution containing 0.1% DMSO (narrow lines).

NMe_3OAc, P_2-SO_3NH_4 and **P_2-Suc** possess polar aromatic substituents directly bonded to the porphyrin *meso*-positions, thus steric interactions force these aryl substituents to twist out of conjugation with the porphyrin. In the second group, dimers **P_2C_2-NMeI** and **P_2C_2-CO_2NH_4**, the terminal aromatic groups are instead conjugated via an acetylene bridge, thereby increasing the length of the π-system. All the compounds exhibit sharp absorption and fluorescence bands in 0.5% pyridine/DMF and DMSO solutions (Fig. 2). Their lowest energy absorption maxima, Q-bands, lie between 650 and 800 nm and are intense compared to those of monomeric porphyrins.[5,30]

The greater degree of conjugation in **P_2C_2-NMeI** and **P_2C_2-CO_2NH_4**, is clearly reflected in the shift of their Q-band absorption and fluorescence maxima to lower energy. The absorption of the conjugated dimers favourably compares with the existing second generation PDT sensitisers, *e.g.* $\varepsilon \approx 4 \times 10^4$ cm^{-1} M^{-1} for Foscan® at 654 nm, for chlorin e6 at 664 nm and verteporfin at 690 nm.[5] The greater near-IR extinction coefficients of the new dimers, compared to the second generation PDT photosensitisers, indicate that they have potential as one-photon PDT agents.

The absorption spectra of the dimers in aqueous solution are broader and less intense than in organic solvents, as exemplified by **P_2-NMe_3OAc** in Fig. 3. In addition, upon going from DMSO to an aqueous environment the fluorescence spectra shift to longer wavelengths and broaden, as shown in Table 1 and Fig. S1, ESI. These changes are consistent with partial aggregation of the conjugated dimers in aqueous solution, which could lead to accelerated relaxation of the excited state by internal conversion.

We tested the photophysical behaviour of the dimers under model physiological conditions by recording a series of fluorescence spectra in aqueous solution at pH 7 following addition of bovine serum albumin (BSA) (Fig. 4 and Table 1). BSA has hydrophobic pockets

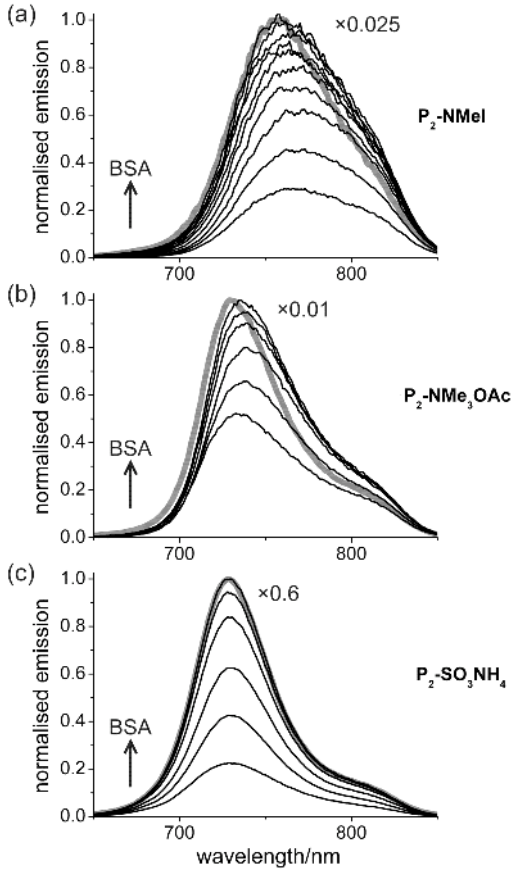

Fig. 4 Fluorescence spectra recorded for solutions of (a) **P_2-NMeI**, (b) **P_2-NMe_3OAc** and (c) **P_2-SO_3NH_4** in water (1 μM concentration) following the addition of aliquots of BSA up to 8 equivalents. The bold grey lines show normalised emission spectra recorded following heating of the resulting 1:8 [dimer]:[BSA] solution at 40°C for 30 min; the normalisation factors are shown in each case (e.g. ×0.6 in c).

which bind non-covalently to a range of drugs[31] and luminescent labels,[32] and binding reduces the aggregation of porphyrin photosensitisers.[33] A marked increase in emission intensity is observed following titration with BSA for all the dimers except **P_2** and **P_2-Suc**. The protein-assisted disaggregation process is accelerated by heating. A further increase in emission intensity is observed when 1 μM solutions containing an 8-fold excess of BSA are maintained at 40 °C for 30 min (close to tissue culture conditions); see ϕ_f with BSA and heat, Table 1. The increase in intensity is accompanied by the narrowing of the emission spectra, Fig. 4, which is also characteristic of disaggregation.

In contrast to the cationic dimers and anionic dimer **P_2C_2-CO_2NH_4**, the spectral shape of the fluorescence peak from the

Table 1 Photophysical parameters of the conjugated porphyrin dimers under a rage of solvent conditions.

	P_2	P_2-NMeI	P_2C_2-NMeI	P_2-NMeOAc	P_2-SO_3NH_4	P_2C_2-CO_2NH_4	P_2-Suc
λ_{max}(em) DMSO	700	730	795	715	715	760	720
λ_{max}(em) H_2O	712	760	800	733	725	780	729
ϕ_f, MeOH[a]	0.11	0.11	0.01	0.10	0.13	<0.001	0.06
ϕ_f, D_2O[b] 0.5% DMSO	<0.001	0.002	<0.001	0.005	0.03	<0.001	0.008
ϕ_f, D_2O/BSA+heat	<0.001	0.08	0.02	0.05	0.05	0.01	0.01
ϕ_Δ, MeOH[c]	0.89	0.54	0.60	0.70	0.69	0.20	0.87
ϕ_Δ, D_2O[d]	0.14	0.50	0.25	0.36	0.59	0.24	0.43

λ_{max}(em) is the peak fluorescence wavelength; ϕ_f is the fluorescence quantum yield; ϕ_Δ is the singlet oxygen quantum yield. [a] *vs.* Chl*a* in ether (0.32),[34] 10% error; [b] *vs.* verteporfin in D_2O (0.05),[35] 10% error; [c] *vs.* Chl*a* (0.77) and $[Ru(bpy)_3]^{2+}$ (0.8),[6] 10% error; [d] *vs.* TMPyP (ϕ_Δ = 0.74)[6] 10% error.

sulfonated dimer **P_2-SO_3NH_4** does not significantly change following heating with BSA, Fig. 4c. In addition, its fluorescence intensity increases by a factor of 1.7, which is considerably less than for the positively charged dimers, that increase more than 10-fold upon heating in the presence of BSA, see Table 1, Fig. 4. This indicates that **P_2-SO_3NH_4** aggregates to a lesser degree in water than the other dimers, which is explained by its structure. **P_2-SO_3NH_4** has twice the number of charges compared to **P_2-NMeI, P_2-NMe_3OAc, P_2C_2-NMeI** and **P_2-Suc**, and its sulfonate groups are much weaker bases than the carboxylate groups of **P_2C_2-CO_2NH_4**, therefore, at neutral pH, it will be fully ionised. Thus **P_2-SO_3NH_4** appears to be the most water-soluble photosensitiser in the series.

Singlet Oxygen Quantum Yields

The singlet oxygen quantum yields of all the porphyrin dimers in methanol and in D_2O are given in Table 1. High quantum yields, greater than 0.5, are obtained in methanol for all the dimers except **P_2C_2-CO_2NH_4**, which could be explained by aggregation of this compound in methanol, as judged from the broadened shape of its absorption spectrum and low fluorescence quantum yield (see Fig. S2, ESI).[36]

The singlet oxygen yields of the dimers in aqueous solution are reduced compared to those in organic solvents, consistent with partial aggregation. Such a reduction in singlet oxygen production efficiency is common upon going from organic solvents to aqueous environments for hydrophobic photosensitisers, *e.g.* for Photofrin® ϕ_Δ is 0.83 in methanol and 0.25 in D_2O.[6] In spite of the partial aggregation in aqueous solution of all the dimers, they show appreciable singlet oxygen yields, intermediate between the clinical sensitisers aluminium disulfonated phthalocyanine ($\phi_\Delta = 0.15$)[37] and verteporfin ($\phi_\Delta = 0.80$).[35]

Two-Photon Absorption Spectra

Hydrophobic conjugated porphyrin dimers have been previously shown to have large peak two-photon cross-sections of 3,000–10,000 GM,[20,26,27,38] several hundred times more than the values characteristic of monomeric porphyrins.[15] The TPA spectra of the ionic dimers were determined by detecting the upconverted fluorescence following excitation between 830–1100 nm, as shown in Fig. 5 and Table 2. The characteristic quadratic dependence of the emission intensity on the laser power was detected at wavelengths longer than 830 nm for **P_2-NMeI, P_2-NMe_3OAc** and **P_2-Suc**, >850 nm for **P_2C_2-CO_2NH_4** and > 900 nm for **P_2C_2-NMeI**. Dimers **P_2-NMeI, P_2-NMe_3OAc** and **P_2-Suc** have peak TPA cross-sections of around 9000 GM between 830–838 nm, whilst the extended π-systems of **P_2C_2-NMeI** and **P_2C_2-CO_2NH_4** result in a further increase to 17000 GM at 916 nm and 14000 GM at 878 nm respectively. This is consistent with previous reports,[39,40] which find that TPA cross-sections rise with increasing electronic conjugation. An additional factor which could contribute to the enhanced δ values for all dimers is that the terminal charged aryl groups are electron-acceptors.

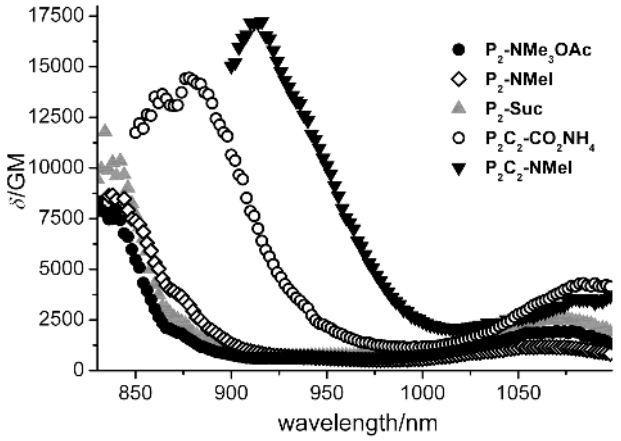

Fig. 5 Two-photon absorption spectra of the dimers measured in DMF with 1% pyridine; **P_2-NMeI** (◇ open diamond), **P_2C_2-NMeI** (▼ black triangle), **P_2-NMe_3OAc** (● black circle), **P_2C_2-CO_2NH_4**. (○ open circle), **P_2-Suc** (▲ grey triangle).

Table 2 Extinction coefficients (ε_{max}) at the Soret band and peak TPA cross-sections (δ_{max}) measured in DMF with 1% pyridine.

compound	OPA λ_{max} (nm)	Log ε_{max}	TPA λ_{max} (nm)[a]	δ_{max} (GM)
P_2-NMeI	458	5.31	838[a]	8,700
P_2C_2-NMeI	471	5.45	916	17,000
P_2-NMeOAc	455	5.36	830[a]	8,300
P_2C_2-CO_2NH_4	463	5.57	878	14,000
P_2-Suc	460	5.40	838[a]	10,000
P_2'[b]	482	5.62	830	5,500
P_2C_2-THS[b]	458	5.48	873	9,100
verteporfin	430	4.98	930	50

[a] TPA λ_{max} is the wavelength at which the highest recorded TPA cross-section is measured; [b] from ref 26 in CH_2Cl_2 with 1% pyridine.

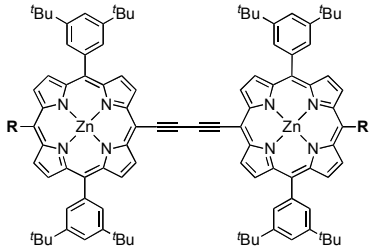

P_2' R = H
P_2C_2-THS R = $C_2Si(C_6H_{13})_3$

Direct comparison with the previously reported conjugated dimers **P_2'** and **P_2C_2-THS**[26] shows that the TPA cross-sections are increased for all the ionic dimers, Table 2. This increase must be due to the terminal charged aryl groups, all of which are electron-acceptors. The greatest increase is observed in **P_2C_2-NMeI** and **P_2C_2-CO_2NH_4**, where the electron-accepting groups are fully conjugated to the porphyrin dimer core forming 'acceptor-π-donor-π-acceptor' systems of the type which generally enhances two-photon absorption.[41]

The TPA cross-sections of this series of conjugated porphyrin dimers compare favourably with the values of other potential photosensitisers designed for two-photon excited PDT. For example, TPA cross-sections of *ca* 2000 GM have been reported for tetraphenyl-porphycenes (determined via two-photon excited singlet oxygen detection),[18] *ca* 1000 GM for porphyrin-TPA chromophore assemblies (determined via two-photon excited fluorescence, similar to the present work)[19] and 7900 GM for self-assembled porphyrin dimers (determined by the *z*-scan technique).[24]

The high TPA efficiencies of our porphyrin dimers within the 'therapeutic window' of biological tissues (700–950 nm)[4] in combination with the high singlet oxygen quantum yields highlight these compounds as promising photosensitisers for two-photon excited PDT.

Intracellular Localisation

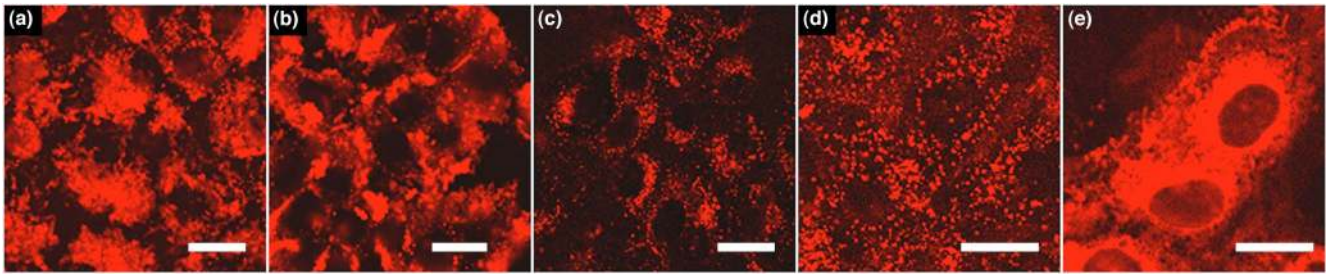

Fig. 6 Confocal fluorescence images (λ_{em} = 650–750 nm) obtained following incubation of SK-OV-3 cells with 10 μM solution of dimers (a) **P_2-NMeI**, (b) **P_2-NMe_3OAc**, (c) **P_2-SO_3NH_4** and (d) **P_2-Suc** for 24 hours and (e) verteporfin for 2 hours. Scale bar 20 μm.

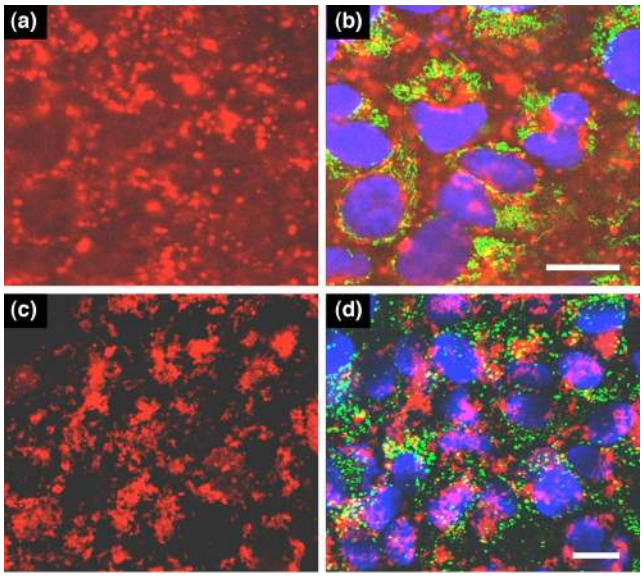

Fig. 7 Confocal fluorescence images obtained following 24 hour incubation of SK-OV-3 cells with 10 μM solution of (a, b) **P_2-NMeI** and (c, d) **P_2-NMe_3OAc**; co-stained with Hoechst 3360 (blue) and either, rhodamine 123 (b, green, mitochondria) or Lysotracker® yellow (d, green, lysosomes). No significant overlap of dimer fluorescence with fluorescence of the organelle trackers is observed. Scale bar 20 μm.

Efficient delivery of the photosensitiser to cells is vital for PDT. Confocal fluorescence microscopy was used to monitor the uptake and intracellular localisation of the new dimers. For this purpose solutions of all the dimers in DMSO (1 mM) were diluted 100-fold into cell culture medium and incubated with SK-OV-3 cells for 1–24 hours. All the ionic porphyrin dimers accumulate inside SK-OV-3 cells.[42] Typical fluorescence images of confluent layers of cells incubated with the dimers are shown in Fig. 6, for the cationic dimers (a) **P_2-NMeI** and (b) **P_2-NMe_3OAc** and the anionic dimers (c) **P_2-SO_3NH_4** and (d) **P_2-Suc**. For comparison an image is also included of cells incubated with the clinical photosensitiser verteporfin (Fig. 6e).

Co-staining experiments using the organelle stains rhodamine 123 (mitochondria) and Lysotracker® yellow (lysosomes) were performed in order to determine the subcellular regions targeted by the dimers, Fig. 7 and Figs S5 and S6, ESI. These probes were chosen since the dimers exhibit punctate fluorescence (Fig. 6), which is typical of the small, granular lysosomes and mitochondria of SK-OV-3 cells. We observed no co-localisation of the dimers with the rhodamine 123 stain and only partial overlap with Lysotracker® yellow. In addition, SK-OV-3 cells were incubated for 4 or 18 hours with dimer **P_2-NMe_3OAc** and then co-stained with the Lysotracker (Fig. S7, ESI). The images indicate that the intracellular distribution of **P_2-NMe_3OAc** may alter over time; these subtle changes are currently the subject of further investigation. While unique colocalisation is not seen with any of the stains following 4 hours incubation, some overlap is evident with Lysotracker yellow after 18 hours, as indicated by the yellow regions in the images. The possibility of multiple localisation domains of **P_2-NMe_3OAc** is illustrated in detail in Fig. S7, ESI, where a series of images are shown through the depth of a cell layer which has been incubated with **P_2-NMe_3OAc** for 24 hours.

Rates of Cellular Uptake

The SK-OV-3 cells were incubated with 10 μM solutions of the dimers and the intensity of the intracellular fluorescence at 650–750 nm was monitored as a function of incubation time, Fig. 8. The rate of increase of the emission appears to depend on the charge of the dimers. Thus the anionic dimer **P_2-SO_3NH_4** reaches maximal cellular fluorescence intensity after incubation for only 4 hours, whereas the cationic dimers take about 20 hours to reach their maximum fluorescence intensities. The curves in Fig. 8 are normalised, so they do not provide information on the final concentration of the dye in the cells. The intensities of the intracellular fluorescence can be compared for pairs of dimers with similar spectral characteristics, such as dimers **P_2-NMeI** and **P_2-SO_3NH_4** (established from solution measurements, Table 1 and Fig. S1, ESI). The intracellular fluorescence intensities of the positively charged dimers **P_2-NMeI** and **P_2-NMe_3OAc** are about five times greater than that of the corresponding negatively charged dimer, **P_2-SO_3NH_4** , indicating that

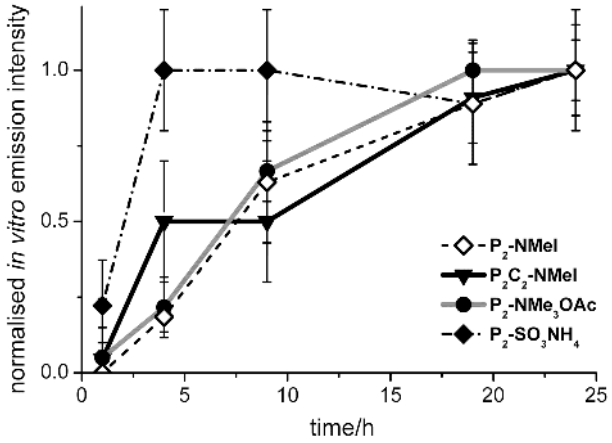

Fig. 8 The uptake curves obtained from the fluorescence images of SK-OV-3 cells incubated with 10 μM solution of ionic dimers **P_2-NMeI** (◇ open diamond), **P_2C_2-NMeI** (▼ black triangle), **P_2-NMe_3OAc** (● black circle) or **P_2C_2-SO_3NH_4**. (◆ black diamond).

the cationic dyes are the more promising photosensitisers.

Photobleaching in Cells

Photostability is an important factor affecting PDT efficiency; a stable photosensitiser can undergo a greater number of excitation events, thereby producing more singlet oxygen, before it is degraded. To determine the *in vitro* photostabilities of the conjugated dimers, we have compared the rates of photobleaching of **P_2-NMeI, P_2-NMe_3OAc** and **P_2-Suc**, which have similar absorption spectra. A confluent layer of cells was incubated with 10 μM of the dimer for 24 hours prior to irradiation with 1 mW of 488 nm laser light (50 sec/scan). The changes in the intracellular fluorescence intensities of **P_2-NMeI, P_2-NMe_3OAc**, **P_2-Suc** and verteporfin are shown in Fig. 9 as function of exposure time. A typical series of confocal fluorescence images obtained during these experiments is given in Fig. S9, ESI. Although the extinction coefficient of verteporfin (11 mM^{-1} cm^{-1}) is an order of magnitude less than that of the porphyrin dimers **P_2-NMeI, P_2-NMe_3OAc** and **P_2-Suc** (160 mM^{-1} cm^{-1} ± 10%) at 488 nm in DMSO, verteporfin photobleaches significantly faster than any of the dimers. Photostability increases in the order: verteporfin < **P_2-NMe_3OAc** < **P_2-Suc** < **P_2-NMeI**. It was established by necrotic cell staining using SYTOX® green that under the conditions used, less than 150 s of irradiation were sufficient to induce cell death with all the photosensitisers tested.[43] Thus the photobleaching of **P_2-NMeI, P_2-NMe_3OAc** and **P_2-Suc** does not appear to significantly interfere with their *in vitro* photodynamic action.

The confocal images collected for **P_2-NMeI** after the photobleaching experiment indicate that the overall intensity of the intracellular fluorescence increases following 488 nm irradiation, Fig. S10, ESI. This observation could be explained by a redistribution of the photosensitiser after irradiation. Such behaviour has been previously observed for several PDT photosensitisers[44-47] including aluminium sulfonated phthalocyanines and Foscan®.[45,46]

The confocal fluorescence images of cells incubated with **P_2-NMe_3OAc**, recorded before and after photobleaching, Fig. 9 (b, c) show that the dimer within the cell layer does not bleach homogeneously. In combination with the observation of biexponential photobleaching kinetics, this suggests that dimer **P_2-NMe_3OAc** displays different photobleaching rates according to its intracellular localisation.

Conclusions

We have analysed a series of new hydrophilic conjugated porphyrin dimers and investigated the photophysical properties relevant to one-photon and two-photon PDT, both in organic solvents and aqueous environments. These dimers show high singlet oxygen quantum yields (0.5–0.9 in methanol), as is desirable for PDT, and exhibit fluorescence in the far-red spectral region 700–800 nm which could be utilised for diagnosis. The ionic dimers investigated here exhibit exceptionally large peak TPA cross-sections of 8,000–17,000 GM at wavelengths accessible with commercial femtosecond lasers, making them extremely promising for two-photon excited PDT. In addition, their red shifted Q-bands (650–800 nm) have high extinction coefficients, *ca* 10^5 cm^{-1} M^{-1}, making them promising for deep tissue penetrating one-photon PDT. We have demonstrated through fluorescence imaging that the dimers efficiently partition into human cancer cells (SK-OV-3). The intracellular fluorescence intensities of the cationic dimers significantly exceed those of the anionic dimers, indicating greater uptake. We have also shown that the dimers are more photostable than the clinical photosensitiser verteporfin, while inside SK-OV-3 cells.

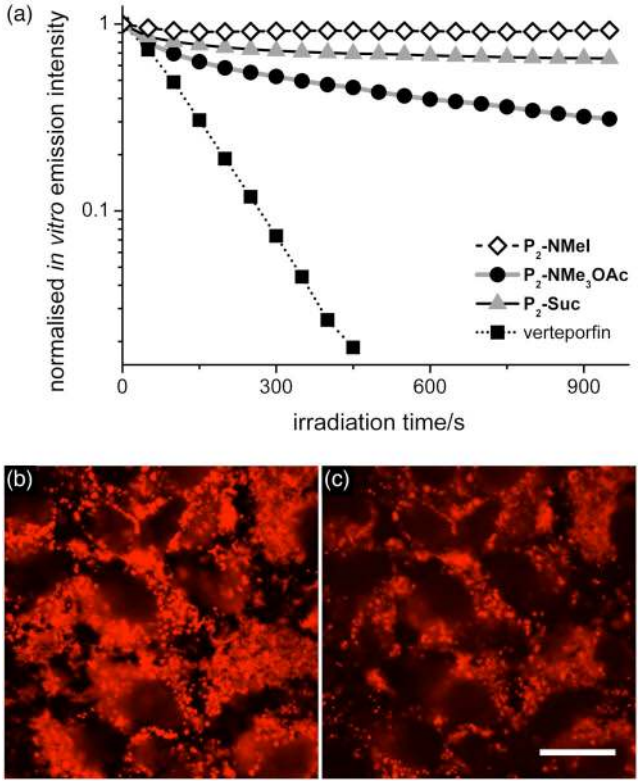

Fig. 9 (a) The changes in the intracellular fluorescence following 488 nm laser irradiation of the confluent layer of SK-OV-3 cells incubated with the 10 μM solution of **P_2-NMeI** (◇ open diamond), **P_2-NMe_3OAc** (● black circle), **P_2-Suc** (▲ grey triangle) and verteporfin (■ black square) for 24 hours. The initial intensity of fluorescence is normalised. Images (b) and (c) show confocal fluorescence images of cells incubated with **P_2-NMe_3OAc** (b) before and (c) after photobleaching under these conditions (900 s irradiation, 488 nm, 1 mW; scale bar 20 μm). The irradiation time required to kill the cells is less than 150 s.

We expect that the phototoxicity of these charged dimers will be largely determined by a combination of their singlet oxygen yields and cellular accumulation (concentration and localisation) behaviour. We present a systematic study of the PDT efficiencies of these new photosensitisers towards a human cancer cells in a following article.[43]

Experimental

Spectroscopic grade D_2O, methanol, DMSO and pyridine (Aldrich) were used for all the measurements. Air-saturated solutions were used for singlet oxygen yield determination. The emission spectra were recorded on a SPEX FluoroLog 3 spectrofluorimeter equipped with a Xenon lamp as an excitation source, and are not corrected for detector sensitivity at λ > 800 nm, which may result in some distortion to the long-wavelength regions of the emission spectra in Figs 2b, 5 and 4.

Singlet oxygen ($^1O_2$) generation was detected by its phosphorescence at 1270 nm using a North Coast Scientific EO-817P germanium photodiode detector. A frequency-tripled Nd:YAG (Continuum Surelite I-10) pumped dye laser (Lambda Physik, Coumarin 120 laser dye) was used as the excitation source providing 0.01–1.0 mJ per pump pulse at the sample between 430–470 nm, with a pulse duration of around 10 ns. The $^1O_2$ quantum yields (ϕ_Δ) were calculated by a comparative method using chl*a* (ϕ_Δ = 0.77) and

$[Ru(bpy)_3]^{2+}$ (ϕ_Δ = 0.80) in methanol, and TMPyP (ϕ_Δ = 0.74) in water as standards.[6] The fluorescence quantum yields were determined relative to chl*a* (ϕ_f = 0.32 in ether)[34] and verteporfin (ϕ_f = 0.05 in D_2O).[35]

The two-photon absorption properties were determined as reported previously,[48] by means of monitoring the fluorescence intensity. Briefly, freshly prepared samples of the dimers in DMF containing 1% pyridine (*ca* 1 μM in 1 cm cuvette) were excited using linearly polarised light from a tuneable femtosecond optical parametric amplifier (TOPAS, Quantronix). The up-converted fluorescence was recorded as a function of excitation wavelength, using a 90° detection geometry and an imaging spectrometer (Triax 550, Jobin-Ivon). The spectra were corrected for the wavelength dependence of the photon flux, pulse duration and beam spatial profile. The spectra were scaled to the cross-section (δ), measured at a selected wavelength. For the δ measurement, we compared the intensities of the one- and two-photon excited fluorescence under the same conditions of registration and similar geometry of excitation.[48]

Imaging was performed using a confocal laser scanning microscope (Leica TCS SP2), coupled to a CW argon-ion laser (488 nm). The fluorescence emission of the photosensitisers in the cells was spectrally dispersed using a prism and detected using a photomultiplier tube. Either dry 40× (*NA* = 0.75) or water immersion 63× objectives (*NA* = 1.23) were used to image. The human ovarian carcinoma cells (SK-OV-3, ECACC) were grown in Dulbecco's modified Eagle's medium (DMEM, Gibco) supplemented with 100 U mL^{-1} penicillin (Sigma), 100 μg mL^{-1} streptomycin (Sigma) and 10% fetal bovine serum (Sigma). The cells were maintained at 37 °C in a humidified 5% CO_2 atmosphere. For the imaging experiments, the cells were seeded at 10^4 cells per well in 0.2 mL of culture medium in untreated 8-well coverglass chambers (Lab-Tek™, Nunc) and allowed to grow to confluence for 24 h. The culture media was replaced with the medium containing the porphyrin dimers and incubated for 1–24 h. Following incubation, the chambers were washed twice with PBS and images were collected at 25 °C. The mean fluorescence intensities from the images were obtained at different incubation times and plotted to determine the rate of uptake of the dimers into cells.

Acknowledgements

We thank EPSRC for financial support. This work was partially supported by the European Union in the form of a Marie Curie individual Fellowship to M.B. under the contract MEIT-CT-2006-041522. E.D. thanks the Wenner-Gren Foundations and the Hans Werthén Foundation (Sweden) for financial support.

Notes and references

1 R. Bonnett, *Chemical Aspects of Photodynamic Therapy*, Gordon and Breach Science Publishers, Amsterdam, 2000.
2 T. J. Dougherty, C. J. Gomer, B. W. Henderson, G. Jori, D. Kessel, M. Korbelik, J. Moan and Q. Peng, *J. Nat. Canc. Inst.*, 1998, **90**, 889; I. J. MacDonald and T. J. Dougherty, *J. Porphyrins Phthalocyanines*, 2001, **5**, 105.
3 M. R. Hamblin and T. Hasan, *Photochem. Photobiol. Sci.*, 2004, **3**, 436.
4 J. Eichler, J. Knof and H. Lenz, *Radiat. Environ. Biophys.*, 1977, **14**, 239; B. C. Wilson, W. P. Jeeves, D. M. Lowe and G. Adam, *Progr. Clin. Biol. Res.*, 1984, **170**, 115; H. Jelínková, J. Pašta, J. Šulc, M. Němec and R. Koranda, *Laser Phys. Lett.*, 2005, **2**, 603.
5. G. Jori, *J. Photochem. Photobiol. B-Biol.*, 1996, **36**, 87.
6. F. Wilkinson, W. P. Helman and A. B. Ross, *J. Phys. Chem. Ref. Data*, 1995, **24**, 663.
7. N. L. Oleinick, R. L. Morris and T. Belichenko, *Photochem. Photobiol. Sci.*, 2002, **1**, 1.
8. R. W. Redmond and I. E. Kochevar, *Photochem. Photobiol.*, 2006, **82**, 1178.
9. J. Dahle, O. Kaalhus, J. Moan and H. B. Steen, *Proc. Natl. Acad. Sci. U. S. A.*, 1997, **94**, 1773.
10 J. D. Bhawalkar, N. D. Kumar, C. F. Zhao and P. N. Prasad, *J. Clin. Laser Med. Sur.*, 1997, **15**, 201.
11 R. L. Goyan and D. T. Cramb, *Photochem. Photobiol.*, 2000, **72**, 821.
12 W. G. Fisher, W. P. Partridge, C. Dees and E. A. Wachter, *Photochem. Photobiol.* **1997**, 66, 141.
13 H. van den Bergh, *Semin. Ophthalmol.*, 2001, **16**, 181.
14 H. van den Bergh, J. P. Ballini and M. Sickenberg, *J. Fr. Ophthamol.*, 2004, **27**, 75.
15 A. Karotki, M. Khurana, J. R. Lepock and B. C. Wilson, *Photochem. Photobiol.*, 2006, **82**, 4432.
16 M. Khurana, H. A. Collins, A. Karotki, H. L. Anderson, D. T. Cramb and B. C. Wilson, *Photochem. Photobiol.*, 2007, **83**, 1441.
17 K. S. Samkoe, A. A. Clancy, A. Karotki, B. C. Wilson and D. T. Cramb, *J. Biomed. Opt.*, 2007, **12**, 14.
18 J. Arnbjerg, A. Jiménez-Banzo, M. J. Paterson, S. Nonell, J. I. Borrell, O. Christiansen and P. R. Ogilby, *J. Am. Chem. Soc.*, 2007, **129**, 5188.
19 M. Drobizhev, F. Q. Meng, A. Rebane, Y. Stepanenko, E. Nickel and C. W. Spangler, *J. Phys. Chem. B*, 2006, **110**, 9802.
20 M. Drobizhev, Y. Stepanenko, Y. Dzenis, A. Karotki, A. Rebane, P. N. Taylor and H. L. Anderson, *J. Am. Chem. Soc.*, 2004, **126**, 15352.
21 I. Hisaki, S. Hiroto, K. S. Kim, S. B. Noh, D. Kim, H. Shinokubo and A. Osuka, *Angew. Chem. Int. Ed.*, 2007, **46**, 5125.
22 A. Karotki, M. Kruk, M. Drobizhev, A. Rebane, E. Nickel and C. W. Spangler, *IEEE J. Sel. Top. Quantum Electron.*, 2001, **7**, 971.
23 M. K. Kuimova, M. Hoffmann, M. U. Winters, M. Eng, M. Balaz, I. P. Clark, H. A. Collins, S. M. Tavender, C. J. Wilson, B. Albinsson, H. L. Anderson, A. W. Parker and D. Phillips, *Photochem. Photobiol. Sci.*, 2007, **6**, 675.
24 K. Ogawa, H. Hasegawa, Y. Inaba, Y. Kobuke, H. Inouye, Y. Kanemitsu, E. Kohno, T. Hirano, S. Ogura and I. Okura, *J. Med. Chem.*, 2006, **49**, 2276.
25 L. Beverina, M. Crippa, M. Landenna, R. Ruffo, P. Salice, F. Silvestri, S. Versari, A. Villa, L. Ciaffoni, E. Collini, C. Ferrante, S. Bradamante, C. M. Mari, R. Bozio and G. A. Pagani, *J. Am. Chem. Soc.*, 2008, **130**, 1894.
26 M. Drobizhev, Y. Stepanenko, Y. Dzenis, A. Karotki, A. Rebane, P. N. Taylor and H. L. Anderson, *J. Phys. Chem. B*, 2005, **109**, 7223.
27 M. Drobizhev, Y. Stepanenko, A. Rebane, C. J. Wilson, T. E. O. Screen and H. L. Anderson, *J. Am. Chem. Soc.*, 2006, **128**, 12432.
28 H. A. Collins, M. Khurana, E. H. Moriyama, A. Mariampillai, E. Dahlstedt, M. Balaz, M. K. Kuimova, M. Drobizhev, Victor X. D. Yang, D. Phillips, A. Rebane, B. C. Wilson and H. L. Anderson, *Nature Photonics*, 2008, **2**, 420.
29 M. Balaz, H. A. Collins, E. Dahlstedt and H. L. Anderson, *Org. Biomol. Chem.*, 2008, submitted.
30 H. L. Anderson, *Chem. Commun.* 1999, 2323.
31 C. Bertucci and E. Domenici, *Curr. Med. Chem.*, 2002, **9**, 1463; J. Ghuman, P. A. Zunszain, I. Petitpas, A. A. Bhattacharya, M. Otagiri and S. Curry, *J. Mol. Biol.*, 2005, **353**, 38.
32 G. Hungerford, K. Suhling, and M. Green, *Photochem. Photobiol. Sci.* 2008, **7**, 734.
33 K. Lang, J. Mosinger and D. M. Wagnerová, *Coord. Chem. Rev.*, 2004, **248**, 321.
34 G. Weber and F. W. Teale, *Trans. Faraday Soc.*, 1957, **53**, 646.
35 B. Aveline, T. Hasan and R. W. Redmond, *Photochem. Photobiol.*, 1994, **59**, 328.
36 The singlet oxygen lifetime obtained following excitation of the conjugated dimers in methanol from the phosphorescence decays at 1270 nm was 11±1 μs, consistent with the literature value of 12 μs, see Fig. S3, ESI. However, the singlet oxygen lifetime obtained following excitation in D_2O formulations varied: for dimers **P_2-SO_3NH_4**, **P_2C_2-CO_2NH_4** and TMPyP 60±5 μs was observed,

consistent with the literature value for D_2O, 65 μs; much shorter lifetime, ca 15 μs, was obtained for other dimers. Fig. S3, ESI shows the typical decay traces obtained at 1270 nm in D_2O. It is known that the singlet oxygen lifetime in DMSO is very short, *ca* 1.8 μs, (A. Kořínek, R. Dědic, A. Molnár, A. Svoboda and J. Hála, *J. Mol. Struct.*, 2005, **744**, 727). We hypothesise that the observed singlet oxygen lifetime in solutions of **P_2**, **P_2C_2-CO_2NH_4** and the positively charged dimers, much shorter than that expected in pure D_2O, is due to quenching by 0.5% DMSO present as solubilising agent.

37 D. Phillips, *Prog. React. Kinet.*, 1997, **22**, 175.

38 A. Karotki, M. Drobizhev, Y. Dzenis, P. N. Taylor, H. L. Anderson and A. Rebane, *Phys. Chem. Chem. Phys.*, 2004, **6**, 7.

39 M. G. Kuzyk, *J. Chem. Phys.*, 2003, **119**, 8327.

40 L. Porrès, O. Mongin, C. Katan, M. Charlot, T. Pons, J. Mertz and M. Blanchard-Desce, *Org. Lett.*, 2004, **6**, 47.

41 M. Albota, D. Beljonne, J. L. Brédas, J. E. Ehrlich, J. Y. Fu, A. A. Heikal, S. E. Hess, T. Kogej, M. D. Levin, S. R. Marder, D. McCord-Maughon, J. W. Perry, H. Röckel, M. Rumi, C. Subramaniam, W. W. Webb, X. L. Wu and C. Xu, *Science*, 1998, **281**, 1653.

42 Confocal fluorescence images of SK-OV-3 cells incubated with **P_2**, using (a) the medium containing 1% DMSO and **P_2**, and (b) **P_2**, in DOPC liposomes are shown in Fig. S4, ESI. However the delivery of **P_2** to the cells is unrelaible under both these conditions.

43 E. Dahlstedt, H. A. Collins, M. Balaz, M. K. Kuimova, M. Khurana, B. C. Wilson, D. Phillips and H. L. Anderson, *Org. Biomol. Chem.*, 2008, submitted.

44 D. Kessel, *Photochem. Photobiol. Sci.*, 2002, **1**, 837.

45 M. Ambroz, A. J. MacRobert, J. Morgan, G. Rumbles, M. S. C. Foley and D. Phillips, *J. Photochem. Photobiol. B-Biol.*, 1994, **22**, 105.

46 A. D. Scully, R. B. Ostler, A. J. MacRobert, A. W. Parker, C. de Lara, P. O'Neill and D. Phillips, *Photochem. Photobiol.*, 1998, **68**, 199.

47 J. W. Snyder, J. D. C. Lambert and P. R. Ogilby, *Photochem. Photobiol.*, 2006, **82**, 177.

48 A. Karotki, M. Drobizhev, M. Kruk, C. Spangler, E. Nickel, N. Mamardashvili and A. Rebane, *J. Opt. Soc. Am. B-Opt. Phys.*, 2003, **20**, 321.